CHALMERS
UNIVERSITY OF TECHNOLOGY

A model platform for solving lithium-ion battery cell data gaps in life cycle assessment

EVS35 Symposium

Oslo, Norway, June 11-15, 2022

A model platform for solving lithium-ion battery cell data gaps in life cycle assessment

Mudit Chordia[1, *], Evelina Wikner[2], Anders Nordelöf[1]

[*]*Corresponding author: mudit@chalmers.se*
[1]*Environmental Systems Analysis, Technology Management & Economics, Chalmers University of Technology*

[2]*Electric Power Engineering, Electrical Engineering, Chalmers University of Technology*

Abstract

With the advent of electromobility, life cycle assessment studies need to keep up with growing number of cell formats and chemistries being adopted for various vehicle applications. This often hindered by lack of data. A model platform is presented, starting with a cell design computation model which is used for calculating the mass of cell components and other design parameters. It also includes a cell performance model, which will link to a battery pack and vehicle model, both used for estimate losses caused by the cell during vehicle operation. Furthermore, the platform comprises a model generating inventory data for life cycle assessment of lithium-ion battery cell production. Together, these parts feed information to life cycle assessment calculations covering both production and use of lithium-ion battery cells. The aim is to support technology development and provide an understanding of how various design changes in cells link to environmental impacts. This conference paper explains model parts and provides exemplary results.

Keywords: Life cycle assessment | Lithium-ion battery | Cell design | Model platform

1 Introduction

Life cycle assessment (LCA) studies analyzing lithium-ion battery (LIB) production vary considerably in their results [1]. One explanation is that the underlying technical scopes are different in terms of chemistries, cell formats and the scale of production. Furthermore, very few studies collect primary inventory data for modeling their LIB product system and instead rely on a limited number of previously published studies. Meanwhile, LIB packs are being implemented in a wide array of applications, including on- and off-road vehicles, ships, and aircrafts. Manufacturers meet the demands of these different applications by adopting different cell geometries and chemistries.

In order for LCA to play a role in guiding this development, and to facilitate a decarbonization of the transport while also minimizing other types of environmental burdens, data must be available to calculate and assess the impacts of LIBs suitable for these different specific applications. However, the current lack of data pertaining to different cell geometries and chemistries hinders from applying LCA with a valid technical representation in many such cases. Consequently, for LCA studies to keep pace with the rapid transition to electromobility and to accurately calculate the environmental impacts of the underlying battery technology, there is a need for new data.

2 Purpose

The overall goal of this work is to develop a model platform for different cell chemistries and formats used in various electromobility applications on the market today, or under development. The model platform outputs a cell specification, including a prediction of the expected performance during operation, and inventory data for LCA with a suitable precision for environmental assessment studies on vehicle or propulsion system level. A physics-based cell model will be developed and linked to an existing LCA inventory model for large scale LIB production, established by Chordia et al. [2]. This is accomplished by coupling the cell design specifications, and its performance when in operation, to changes in the material and energy demands of the cell manufacturing. The overall aim is thus to cover data gaps for LCA of LIBs for a range of electromobility applications and enable assessment of trade-offs between environmental impacts linked to cell production, and impacts linked to its use, when the design is altered.

The purpose of this conference paper is to present the model platform at a conceptual level to illustrate how LIB cell data can be established for use in LCA studies. Additionally, we present the work-in-progress in more detail for how some of the incorporated sub-models have been built, focusing on the cell design computations, some aspects of cell performance, as well as the modifications made to the existing production LCA inventory data model. Example results are presented for two cell designs created by the model platform, one energy optimized and one power optimized cell.

3 Methods

LCA methodology is commonly used in environmental systems analysis studies to measure the environmental performance of products and services. A key characteristic of LCA studies is the definition of a clear goal and scope. The latter refers to the technical, spatial, and temporal boundaries of the system covered, and the selection of environmental impacts to be calculated for the studied system. Additionally, a functional unit is defined that in basic quantitative terms represents the essential function that the studied system is expected to deliver, and in relation to which the environmental impacts are calculated and reported. LCA studies depend on the data collected for building the inventory model that represent the product system. This can be a challenge in the absence of readily available data or gaps in the existing data. For this we used an inter-disciplinary approach to generate usable data for the LCA model and fill data gaps where necessary.

The development of this model platform requires multi-disciplinary collaboration. On the technical design side, it includes computing cell design options and to evaluate their performance, on cell level, as well as on the pack level when operating in an electric vehicle powertrain, by building a set of models in tools such as MatLab, COMSOL Multiphysics and Simulink, and connect these models in one common platform where they exchange information. On the life cycle inventory side, it includes a detailed LIB manufacturing model where single unit process flows are modified along with the cell design variations, and a simpler use phase modeling step, both of which are implemented as one foreground product system in the OpenLCA, and further linked to generic background inventory data from the Ecoinvent database [3]. In the end, results can be extracted in the form of environmental impact assessments of LIB cells for various categories such as contributions to global warming, acidification or use of scarce resources.

3.1 The model platform

Model calculations can start from different known inputs. For example, the platform will be able to estimate a cell design based on manufacturer's tabulated cell data, i.e., cell constituent mass per kWh or share of the total cell mass, or from the desired cell capacity and format. The cell design calculations are made flexible, with the starting point being either a fully specified cell, or only a few known inputs where gaps in the cell specification instead represent typical design selections, i.e., a "general" cell. In such cases, without specific inputs, estimates are based on requirements to reach a target cell capacity, together with the desired formfactor and material selection. Design assumptions and generalised cell data are compiled from reports on commercial cells in literature, cell disassemblies and collaboration with industrial partners.

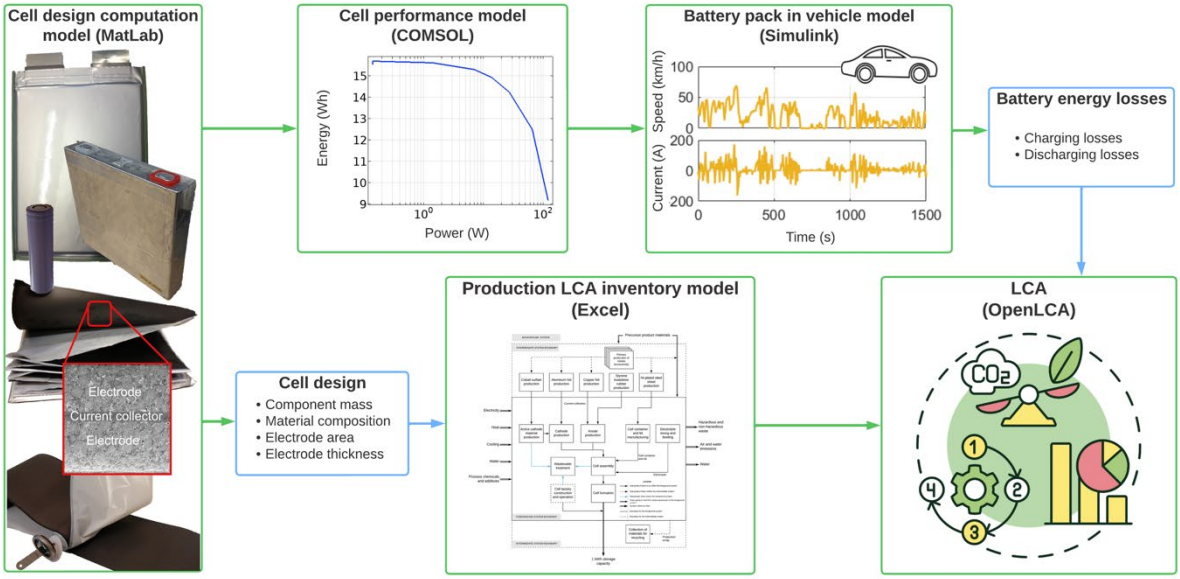

Figure 1: Overview of the model platform, from cell design parameters to LCA calculations.

Expectedly, the precision of the physics-based model in providing estimations of the cell performance at different loads will increase with the amount of specific information provided as input. In a subsequent step, the aim is to couple these results to an electric vehicle powertrain model via an equivalent circuit representation. The complete model platform is visualized in Figure 1. The first block from the left is the cell design computation model in MatLab, further described in Section 3.2, where the cell design is determined based on parameters specified by the operator of the model platform, or from pre-defined type values. The output generated from this first model is sent further in two different streams of information. One becomes direct input for the cell performance model in COMSOL and the other, a list of input parameters for the LCA inventory model for cell production. The role of the cell performance model is to establish information about energy losses from resistance during charging and discharging, and cell energy content, to send further the battery pack and electric vehicle powertrain model in Simulink. The cell performance model is described in Section 3.3, whereas the battery pack in the vehicle model has not been implemented at this stage and remains for future work. It will deliver energy use data representing the operation stage of the battery cell in generalized electric vehicle when operated on a specific drive cycle. In doing so, it will also account for the cell's share of the total vehicle mass, and losses caused by this mass contribution. Finally, information about the total energy losses caused by the cell is applied in the OpenLCA product system model to account for the use phase of the cell.

The other stream of information leaving the cell design computation model contains the cell mass configuration and data for the cell geometry, in turn communicated to the LCA inventory model for the manufacturing stage, constructed in Excel. By parameterizing a cell production model originally established for cylindrical cell production, all relevant energy and material flows in a number of cell production processes are scaled, omitted, or added, to adapt the production inventory data to the desired chemistry and geometry. The production LCA data is then combined with the use phase energy data in OpenLCA product system model to calculate environmental impacts from cell production and use. For the scope of the conference paper, one energy optimized and one power optimized version of a lithium nickel manganese cobalt oxide graphite cell of 21700 format (21700 – NMC811 | graphite) were designed in the cell design computation model, taking a starting point in a "reference cell" design previously investigated by Chordia et al. [2]. To exemplify the kind of information that the complete model platform will output, exemplary results are then reported in Section 4. These include cell design computation output in Section 4.1, cell performance model, energy losses in cell due to internal resistance in Section 4.2 and climate impact assessment results for the production life cycle stage in Section 4.3.

3.2 Cell design computation model

Chordia et al. [2] made the mass composition available for a 21700 – NMC811 | graphite cell, with an estimated capacity of 15.40 Wh/cell. However, no further information about the design of the reference cell was given, and the interior structure and detailed design had to be established via a cell computation model. With this aim, a flexible regime was developed to calculate a cell design based on the expected capacity and the stated geometrical format of the cell. This calculation regime was setup in such a way that if the sought cell capacity cannot be reached in the selected cell format, the maximum and minimum reachable capacities are calculated. For capacities that can be reached within the selected cell format, the cell computation model provides one power optimized and one energy optimized version of each cell design.

These calculations require several parameters that needs to be set by the operator of the model. First, when the script is started, the cell format, size and casing material must be chosen. Next, the electrode active materials are asked for. This is followed by a few design selections for the separator and the composition of active materials. For each parameter, a recommended value is suggested as a default value and a typical range for commercial lithium-ion cells is displayed. Thus, the setup gives an operator the ability to create a vast number of possible cell designs.

The cell design calculation is based on the sought cell capacity. For the 21700 – NMC811 | graphite cell the capacity is calculated from the cell energy over the nominal cell voltage

$$Ah_{cell} = \frac{Wh_{cell}}{V_{nominal}} = \frac{15.4}{3.65} = 4.22\ Ah$$

When constructing a cell, the maximum cell capacity is determined by the positive electrode (PE) capacity as the lithium is stored in the PE material during assembly. The mass of PE active material is calculated from

$$m_{PE,AM} = \frac{Ah_{cell}}{Q_{S,PE} AM_{wt\%} \rho_{PE} U_{\%}}$$

where $Q_{S,PE}$ is the specific capacity, $AM_{wt\%}$the active material wt%, ρ_{PE} the density of the porous electrode, and $U_{\%}$the utilization of the active material. The density of the porous electrode is

$$\rho_{PE} = \rho_{AM}(1 - \varepsilon_l)\, AM_{wt\%}$$

where ε_l is the porosity of the electrode and ρ_{AM} the bulk density of the active electrode material.

The areal capacities are estimated for the cell based in two conditions. One based on a minimum and maximum thickness of the PE (20-300μm), and the second on a maximum and minimum areal capacity for the selected PE commonly seen in commercial LIBs, typically in the range 1-5 mAh/cm^2 for NMC811.

$$ArealCap_{PE} = \begin{cases} \max\{20e^{-6} Q_{S,PE} AM_{wt\%} \rho_{PE} U_{\%},\ \min(ArealCap_{AM})\} \\ \min\{300e^{-6} Q_{S,PE} AM_{wt\%} \rho_{PE} U_{\%}, \max(ArealCap_{AM})\} \end{cases}$$

The areal capacity for the negative electrode (NE) is

$$ArealCap_{NE} = ArealCap_{PE} NP_{ratio}$$

where the NP_{ratio} is the capacity of the NE over the PE capacity. When using graphite as negative electrode this ratio is in the range from 1.1-1.2. The areal capacity for the PE is used to recalculate a max and min

thickness of the porous electrode.

$$d_{PE} = \frac{ArealCap}{Q_{S,PE} AM_{wt\%} \rho_{PE} U_{\%}}$$

The needed electrode area is calculated as

$$A_{PE} = \frac{Ah_{cell}}{2ArealCap_{PE}}$$

where the electrode is assumed to be coated on both sides. The thickness of the double coated electrodes is calculated as

$$d_{Electrode} = 2d_{AM} + d_{cc}$$

where d_{cc} is the current collector foil thickness.

Once the balance between the electrodes has been calculated, the selected format is to be considered. Based on the selected cell format a possible cell area with the different thicknesses of the two electrodes are calculated. For a cylindrical cell the casing is considered to have 0.2 mm thick wall. The Archimedes spiral equation is used to calculate the number of turns, n ,

$$n = \frac{(D - 2d_{can\ wall} - d_{stack} - D_{inner\ void} - D_{outer\ void})/2}{d_{stack}}$$

where the $d_{can\ wall}$ is the casing wall thickness, $D_{inner\ void}$the inner void diameter, $D_{outer\ void}$ the outer void diameter (typically two layers of separator or other insulation material), and d_{stack} it the thickness of the stack for the jelly roll, consisting of one positive and one negative double coated electrode with two layers of separator.

$$d_{stack} = d_{PE,Electrode} + d_{NE,Electrode} + 2d_{sep}$$

The length of the jelly roll is calculated from

$$l_{jr} = \int_0^{n \cdot 2\pi} \sqrt{\left(\frac{D_{inner\ void}}{2} + \frac{d_{stack}\theta}{2\pi}\right)^2 + \left(\frac{d_{stack}}{2\pi}\right)^2}\, d\theta$$

The area of the different components is calculated based on the assumed overhang of the NE and separator, see Figure 2 and Table 3.

$$\begin{cases} A_{PE} = (l_{jr} - L_{NE,UC} - L_{NE,OH})(H - H_{TC} - 2d_{can\ wall} - W_{NE,OH} - W_{sep,OH}) \\ A_{PE,cc} = A_{PE} \\ A_{NE} = (l_{jr} - L_{NE,UC})(H - H_{TC} - 2d_{can\ wall} - W_{sep,OH}) \\ A_{NE,cc} = l_{jr}\left(H - H_{TC} - 2d_{can\ wall} - W_{sep,OH}\right) \\ A_{sep} = 2(l_{jr} + L_{sep,OH})(H - H_{TC} - 2d_{can\ wall}) \end{cases}$$

The available capacity, Q_{cell}, is calculated by the PE areal capacity and area

$$Q_{cell} = ArealCap_{PE} \cdot 2A_{PE}$$

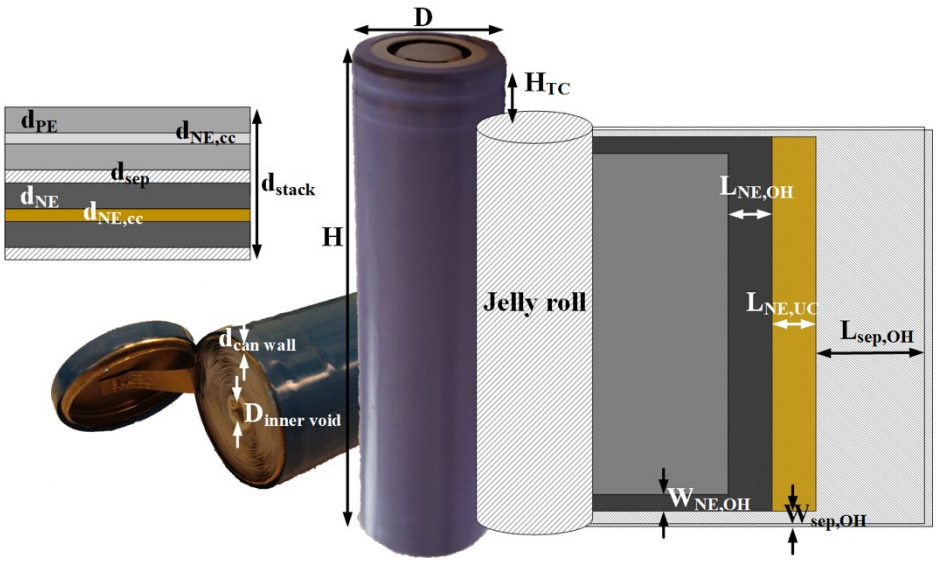

Figure 2. Composition of a cylindrical cell and parameters used for cell design calculations.

The calculated cell capacity is then compared to the sough cell capacity, Ah_{cell}, in a series of steps.

- If $\max(Q_{cell}) < Ah_{cell}$ the code will reply with "The wanted capacity cannot be reached in the selected cell format".
- If $\max(Q_{cell}) > Ah_{cell}$ & $\min(Q_{cell}) > Ah_{cell}$ the code increases the lowest $ArealCap_{PE}$ values in discrete steps until $\min(Q_{cell}) = Ah_{cell}$.
- If $Q_{cell} > Ah_{cell}$ the code scales the area so that $Q_{cell} = Ah_{cell}$.

When the final design of the cell is determined, the masses for all materials in the cell are calculated based on the used volume and density of the materials.

3.3 Cell performance model

The cell performance is simulated by using COMSOL Multiphysics Lithium-ion Battery module that bases on the model derived by Doyle et al. [4]. The full disclosure of the physics-based model will be presented in a later publication. These physics-based models require a large number of cell design parameters as well as material properties. In this first demonstration work the material properties has been taken from COMSOLs material library and cell design parameters from the cell design computation model. In addition to the described calculations above, the volume fraction for the active materials has been estimated by

$$\varepsilon_{AM} = \frac{(AM_{wt\%})}{V\rho_{AM}}$$

where,

$$V = \frac{(AM_{wt\%}/\rho_{AM} + (1 - AM_{wt\%})/\rho_{add})}{(1 - \varepsilon_l)}$$

The cell design parameters used as input for the model can be found in Table 2. In this first stage the model is used to simulate the cell energy and power relation and resistance from pulses at different state of charge (SOC) levels.

3.4 Life cycle assessment model

The scope of the existing LCA inventory model for cell production in Chordia et al. [2] covers the production of 21700 – NMC811 | graphite cells from the cradle, i.e., the mining sites, to the gate of a giga-scale cell factory where the cell is produced. Broadly, this includes the raw material processing, the production of precursors for active materials and other subparts, all the way to cell assembly and cell formation in the cell factory, where they are readied for shipment to the customer. In this work, we have developed the LCA inventory model further such that an estimate for production data such as mass and energy input for other cell designs can be derived based on the reference cell. Mass inputs from the cell design computation model are used in creating specific cell component and assembly unit processes in the LCA model. Specifically for calculating the energy flows, the manufacturing model used in the reference case cell [2] was extrapolated based on the cell properties relating to how each cell subpart is processed or machined in specific manufacturing step. For example, the electricity used in the active cathode material mixing process ("slurry preparation") is proxied to depend on viscosity of the slurry, and a coating process is assumed to depend on the surface area to be coated. This is explained using a generic example.

$E_{ref,\ activity}$ is the energy input for a specific manufacturing process/activity in the reference cell. The specific cell property on which the manufacturing process depends on is given as S_{ref}. Further, based on the cell design computation model, the same cell property identified in a modeled "application cell" is $S_{app,\ property}$. The scaling ratio $R_{property}$, is now defined as the ratio of the given cell property in the application cell to the reference cell.

$$R_{property} = \frac{S_{app,\ property}}{S_{ref}}$$

The final scaling ratio could depend on a number of cell properties. Thus, the final scaling ratio $R_o$is given as

$$R_o = R_{property\ 1} \times R_{property\ 2} \times R_{property\ 3} \cdots$$

Thus, the energy input in the application cell can be calculated as

$$E_{app} = R_O \times E_{ref,\ activity}$$

Thus, for each manufacturing activity in production of the reference cell one or several specific cell properties were identified to enable a linear scaling of how energy use in the factory would change when instead representing the cell design provided by the cell design computation model.

To exemplify results generated from the LCA parts of the model platform, for this conference paper scope, the original 21700 – NMC811 | graphite cell analyzed in Chordia et al. [2] is compared with the two newly generated cell versions of the same type, the energy optimized and power optimized 21700 – NMC811 | graphite cells for climate impacts from the production life cycle stage – using the ReCiPe impact assessment package [5]. The comparison is made for a functional unit of 1 kWh storage capacity.

4 Results

This section presents the results of the analysis conducted in this study. This includes the calculations for cell design, energy losses, and climate change impacts due to cell production.

4.1 Cell design computation output

The cell design computation model provides two different output results: one "mass composition" and one "design specification". In this demonstration, two versions of the 21700-NMC811 | graphite cell with the targeted energy content of 15.4 Wh and cell capacity of 4.22 Ah was computed – one power optimized and one energy optimized version which both fulfill this energy requirement and compared with the original reference cell. The input used for the cell design computation model in this example are reported in Table A1 and A2 of the Appendix. Table A1 specifies input data on the cell level, i.e., format, casing material, separator, and electrolyte parameters. The Table A2 specifies the electrodes. The parameters underlying the calculations for the jelly roll size and the cylindrical casing is included in Table A3.

The resulting mass compositions are presented in Table 1. Although all three versions of the cell have the same material composition in their electrodes, i.e., NMC811 for the positive side (cathode during discharge) and graphite on the negative (anode) side, as well as the same cell type (21700), the mass share of individual cell components are slightly different. Still, the mass composition of the energy optimized cell is very similar the reference cell, which is not surprising as the reference cell is expected to have better energy performance relative to its power performance. The power optimized cell has a higher total mass. As the capacity of the cell is determined by the available capacity in the PE material, both cell designs have the same amount of PE paste. However, a difference can be seen in the PE current collector mass, mass of the NE, and tab compensation. The tab compensation is calculated from the number of tabs that is connected to the jelly roll. In a power optimized cell, it is common to have more than one tab, to distribute the current more evenly in the cell, while energy optimized cells only have a single tab for each electrode in the entire jelly roll, see Figure 2 for illustrations. A power optimized cell has thinner electrode coating, thus a larger electrode surface.

Table 1. Mass composition of the reference cell [2] and the energy and power optimized cells.

	Reference cell		Energy optimized		Power optimized	
Component	**Weight %**	**Weight g**	**Weight %**	**Weight g**	**Weight %**	**Weight g**
Positive electrode / Cathode (during discharge)	**40.0%**	**27.0**	**39.9%**	**26.9**	**38.1%**	**28.1**
- Positive electrode paste	*37.4%*	*25.2*	*37.7%*	*25.4*	*33.2%*	*25.4*
- Positive electrode current collector (foil)	*2.6%*	*1.7*	*2.1%*	*1.4*	*3.6%*	*2.6*
Positive tab compensation (foil)	**0.1%**	**0.1**	**0.1%**	**0.0**	**0.2%**	**0.2**
Negative electrode / Anode (during discharge)	**30.0%**	**20.2**	**29.9%**	**20.1**	**31.8%**	**23.4**
- Negative electrode paste	*22.9%*	*15.5*	*23.8%*	*16.1*	*21.7%*	*16.0*
- Negative electrode current collector (foil)	*7.1%*	*4.8*	*6.0%*	*4.1*	*10.1%*	*7.4*
Negative tab compensation (foil)	**0.3%**	**0.2**	**0.2%**	**0.2**	**0.8%**	**0.6**
Electrolyte	**10.0%**	**6.7**	**11.1%**	**7.5**	**10.2%**	**7.5**
Separator	**1.9%**	**1.3**	**2.1%**	**1.4**	**3.5%**	**2.5**
Cell container assembly	**17.7%**	**11.9**	**16.8%**	**11.3**	**15.4%**	**11.3**
- Cylindrical casing	*12.2%*	*8.2*	*11.5%*	*7.7*	*10.5%*	*7.7*
- Lid	*2.7%*	*1.8*	*2.7%*	*1.8*	*2.4%*	*1.8*
- Fastening tape	*0.9%*	*0.6*	*0.0%*	*0.0*	*0.0%*	*0.0*
- Insulation ring	*1.8%*	*1.2*	*2.7%*	*1.8*	*2.4%*	*1.8*
Total	**100.0%**	**67.5**	**100.0%**	**67.4**	**100.0%**	**73.7**

The second output from the cell design computation model is the design composition. Table 2 shows the list of parameters calculated for the two cell designs. Here, the difference between the two cells area is clearly visible, where the power optimized cell has almost the double area compared to the energy optimized cell.

Table 2. Design specification for the energy and power optimized cells with the targeted 4.22 Ah cell capacity estimated by the cell design computation model. The terms "cathode" and "anode" refers to discharge mode.

Component	Energy optimized	Power optimized
Positive electrode ("cathode") area (m^2)	0.08	0.16
Positive electrode current collector area (m^2)	0.04	0.08
Positive electrode thickness (µm)	79.4	42.3
Positive electrode volume fraction	0.67	0.67
Positive electrode current collector (foil) (µm)	12.0	12.0
Positive electrolyte volume fraction	0.25	0.25
Positive particle diameter (µm)	10.0	10.0
Negative electrode ("anode") area (m^2)	0.09	0.16
Negative electrode current collector area (m^2)	0.05	0.08
Negative electrode thickness (µm)	110	58.7
Negative electrode volume fraction	0.72	0.72
Negative electrode current collector (foil) (µm)	10.0	10.0
Negative electrolyte volume fraction	0.25	0.25
Negative particle diameter (µm)	10.0	10.0
Separator thickness (µm)	15.0	15.0
Separator porosity	0.40	0.40
Areal capacity (A/m^2)	50.0	26.7

4.2 Energy losses in cell due to internal resistance

The cell performance model uses the design composition results in Table 2 as input. Table 3 shows that the simulation results in slightly higher energy content then the target cell energy for both designed cells, 15.7 Wh. However, the simulated capacity is slightly lower than the calculated targeted capacity.

The cells simulated energy and power relation is visualized to the left in Figure 3. The right part of the figure shows the instantaneous resistance as a function of SOC. The power optimized cell has lower resistance and thus better power capabilities compared to the energy optimized cell. Therefore, the power optimized cell will have lower resistive losses when operated with the same current. However, this does not mean that total losses are lower also on pack level. The power optimized cell has larger mass compared to the energy optimized cell, and in vehicle operation the higher overall weight can contribute to higher total losses. In addition, when designing a battery pack several criteria must be considered, including vehicle requirements such as power, energy, weight and volume, as well as the optimal operation point for the cells. The power optimized cell will have a higher optimal operation current compared to the energy optimized cell.

Table 3. Targeted energy and capacity compared to simulated results from the cell performance model for the power and energy optimeized cells.

Targeted cell energy (Wh)	15.4	15.4
Targeted cell capacity (Ah)	4.22	4.22
Simulated capacity 4.2-2.5 V (Ah) | (Ah/m^2)	4.19 | 49.6	4.19 | 26.5
Simulated energy 4.2-2.5 V (Wh) | (Wh/m^2)	15.7 | 186	15.7 | 99.2
Calculated energy density (Wh/l)	635	635
Calculated energy density (Wh/kg)	236	211

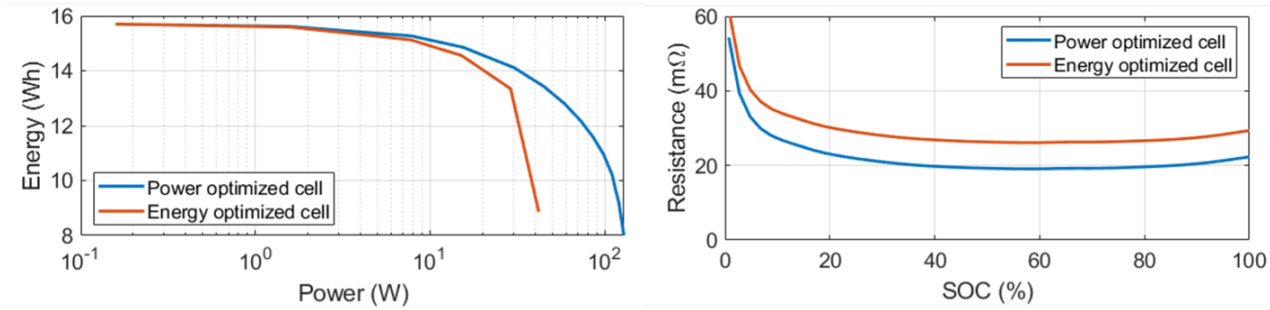

Figure 3: Cell performance simulation results for the energy and power optimized 21700 cells. To the left, the energy and power capabilities and to the right the internal instantaneous resistance values as a function of SOC for the two different cell designs.

4.3 Climate impact assessment results

The cradle-to-gate climate change impacts from cell production are presented in Figure 4. The results are shown specifically for the contributions of the positive and negative electrodes, and all other parts classified in one category. The results cover both upstream processes as well as the activities in the factory for the different parts, meaning that cell assembly and other joint cell burdens are accounted for among "other cell components". Overall, the power optimized cell show higher impacts compared to the energy optimized cell, since it has larger contributions from both electrodes. Firstly, this is due to the higher mass of these parts in the power optimized cell. Secondly, it also requires more energy in production. Even if the coating layers on the electrodes are thicker in the energy optimized cell, the surface areas of the foils are larger in the power optimized cell, resulting in higher energy use during the coating processes.

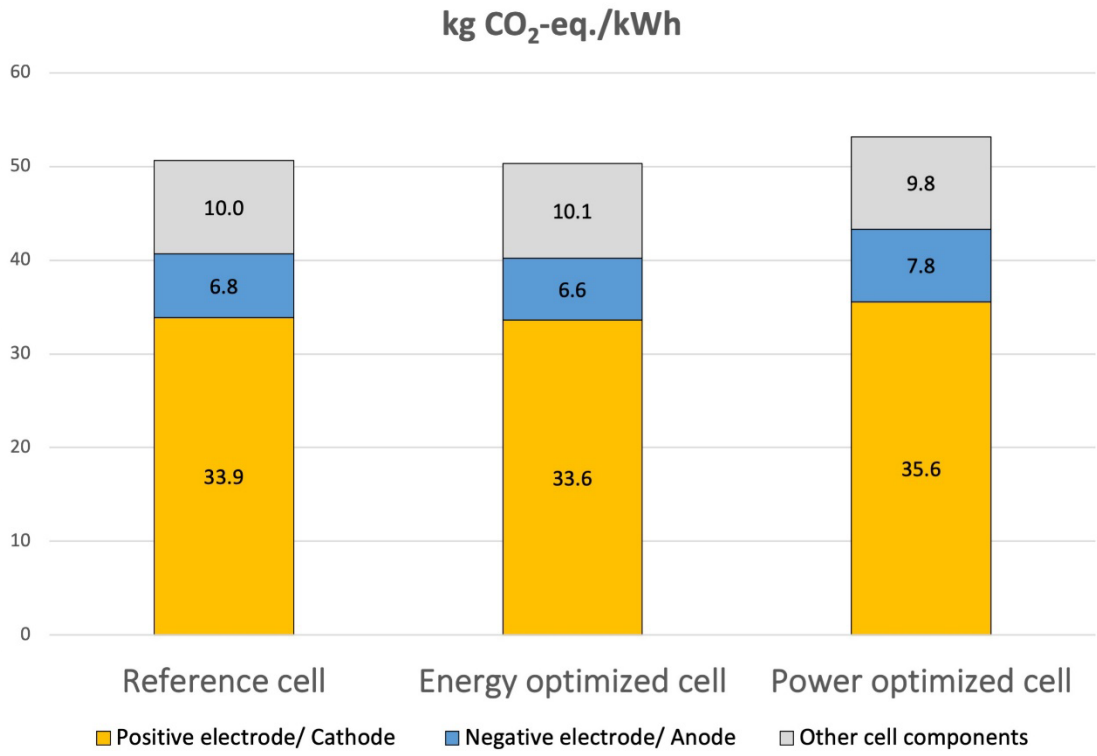

Figure 4: Climate change impacts of the cell design examples benchmarked against the reference cell.

5 Conclusions and future work

A ready-to-use model platform for solving lithium-ion battery cell data gaps in LCA is under development. In its finalized form, the model will be able to compute the design for several cylindrical, prismatic and pouch cell variants, and link this information further to enable LCA covering both production and use of these cells. In this conference paper we have explained the implementation of cell design computation step, and how resistive losses are calculated in the performance model step. It is also explained how the production LCA inventory model is adapted to handle the variations in the design. Results are exemplified for different versions of a 21700-NMC811 | graphite cell, showing how the model can be used and what kind of comparisons that can be made. For example, cells with the same energy content and cell capacity show small, but nevertheless, differences in terms of climate impacts.

Future work includes finalizing the battery pack and vehicle model. It will take the results from the cell performance model to derive an equivalent circuit model for the cell. It will also cover a battery pack design estimation to account for the losses caused by the cell when operating in this battery pack as a part of a generic powertrain for different drive cycles. Further work also includes expanding all model parts such that they can account for more electrode materials and cell formats, for example NMC622 and NMC111 chemistries, varying prismatic and pouch geometries, and other dimensions of cylindrical cells. Finally, the model will be validated, although broad real-world data availability to do this in more than a few sample points, remains a challenge.

Acknowledgments

The authors would like thank Dr. Matthew Lacey (Scania) for productive discussions on cell design and sharing experiences from cell disassemblies, as well as technical support for the cell design calculations. Thanks also to Anastasiia Mikheenkova (Uppsala University) for the SEM picture of an electrode cross section.

References

1. Peters, J.F. and M. Weil, *Providing a common base for life cycle assessments of Li-Ion batteries.* Journal of Cleaner Production, 2018. **171**: p. 704-713.
2. Chordia, M., A. Nordelöf, and L.A.-W. Ellingsen, *Environmental life cycle implications of upscaling lithium-ion battery production.* The International Journal of Life Cycle Assessment, 2021. **26**(10): p. 2024-2039.
3. Wernet, G., et al., *The ecoinvent database version 3 (part I): overview and methodology.* The International Journal of Life Cycle Assessment, 2016. **21**(9): p. 1218-1230.
4. Doyle, M., T.F. Fuller, and J. Newman, *Modeling of Galvanostatic Charge and Discharge of the Lithium/Polymer/Insertion Cell.* Journal of The Electrochemical Society, 1993. **140**(6): p. 1526-1533.
5. Huijbregts, M.A.J., et al., *ReCiPe 2016 : A harmonized life cycle impact assessment method at midpoint and endpoint level Report I: Characterization*, in *ReCiPe 2016 : Een geharmoniseerde levenscyclus impact assessment methode op 'midpoint' en 'endpoint' niveau Rapport 1: karakterisatie*. 2016, Rijksinstituut voor Volksgezondheid en Milieu RIVM.

Appendix

Table A1: Assumption of parameters for the cell design calculations.

Cell format	21700
Cell casing	A3 steal
NP-ratio, NP_{ratio}	1.1
Thickness Separator, d_{sep} [µm]	15
Density Separator, ρ_{sep} [g/cm^3]	1.0
Density electrolyte, ρ_l [g/cm^3]	1.11
Electrolyte capacity ratio, E_{cap} [ml/Ah]	1.6

Table A2: Assumption of parameters for the electrodes.

Parameter	Negative electrode (NE)	Positive electrode (PE)
Active material	Graphite	NMC811
Active material weight fraction, $AM_{wt\%}$ [wt%]	97	96
Porosity, ε_l	0.25	0.25
Foil material	Cupper	Aluminum
Thickness, $d_{Cu/Al}$ [µm]	10	12

Table A4: Parameters for jelly roll and casing calculations.

Can diameter, D [cm]	2.1
Can height, H [cm]	7.0
Term clearance [cm]	0.36
Can thickness, $d_{can\ wall}$ [cm]	0.02
Inner void diameter, $D_{inner\ void}$ [cm]	0.1
Outer void diameter, $D_{outer\ void}$	$2d_{sep}$
Length uncoated NE cc-foil [mm]	3.3
Width NE overhang [cm]	0.05
Length NE overhang [cm]	1.0
Width separator overhang [cm]	0.05
Length separator overhang [cm]	0.6
Number of tabs, Power | Energy	4 | 1
Tab volume [cm^3]	0.017
Density Steal, ρ_{Steal} [g/cm^3]	7.86
Density Aluminum, ρ_{Al} [g/cm^3]	2.70
Density Cupper, ρ_{Cu} [g/cm^3]	8.96
Density Graphite, ρ_G [g/cm^3]	2.24
Density NMC811, ρ_{NMC811} [g/cm^3]	4.87
Top plate mass + insulation ring, [g]	$0.042\rho_{Steal}\pi\left(\frac{D-2d_{can\ wall}}{2}\right)^2+0.7$
Tape and insulation, [g]	1.8

Presenter Biography

Mudit Chordia is a Doctoral researcher at the Division of Environmental Systems Analysis, Chalmers University of Technology, Sweden. Mudit has an academic background in mechanical and petroleum engineering, and industrial ecology. Mudit's broad area of research includes developing an understanding of upscaling lithium-ion battery production and recycling and its implications on upstream battery material supply chain.